

LRH: J.L. HIZZETT ET AL.

RRH: MUD-CLAST ARMORING AND ITS IMPLICATIONS FOR TURBIDITE SYSTEMS

Research Article

DOI: <http://dx.doi.org/10.2110/jsr.2020.35>

Mud-clast armoring and its implications for turbidite systems

JAMIE L. HIZZETT,^{1,2} ESTHER, J. SUMNER,² MATTHIEU J.B. CARTIGNY,³ AND MICHAEL A. CLARE¹

¹ National Oceanography Centre, University of Southampton, Waterfront Campus, Southampton, U.K.

² Ocean and Earth Science, National Oceanography Centre Southampton, University of Southampton, Southampton, U.K.

³ Departments of Earth Science and Geography, University of Durham, Durham, U.K.
e-mail: j.l.hizzett@soton.ac.uk

ABSTRACT: Seafloor sediment density flows are the primary mechanism for transporting sediment to the deep sea. These flows are important because they pose a hazard to seafloor infrastructure and deposit the largest sediment accumulations on Earth. The cohesive sediment content of a flow (i.e., clay) is an important control on its rheological state (e.g., turbulent or laminar); however, how clay becomes incorporated into a flow is poorly understood. One mechanism is by the abrasion of (clay-rich) mud clasts. Such clasts are common in deep-water deposits, often thought to have traveled over large (more than tens of kilometers) distances. These long travel distances are at odds with previous experimental work that suggests that mud clasts should disintegrate rapidly through abrasion. To address this apparent contradiction, we conduct laboratory experiments using a counter rotating annular flume to simulate clast transport in sediment density flows. We find that as clay clasts roll along a sandy floor, surficial armoring develops and reduces clast abrasion and thus enhances travel distance. For the first time we show armoring to be a process of renewal and replenishment, rather than forming a permanent layer. As armoring reduces the rate of clast abrasion, it delays the release of clay into the parent flow, which can therefore delay flow transformation from turbidity current to debris flow. We conclude that armored mud clasts can form only within a sandy turbidity current; hence where armored clasts are found in debrite deposits, the parent flow must have undergone flow transformation farther up slope.

INTRODUCTION

The clay content of submarine sediment density flows is a fundamental control on their rheology and the resulting flow dynamics. However, the mechanisms by which clay is ingested into submarine sediment density flows, particularly by the disaggregation of mud clasts, remain poorly understood. Understanding the dynamics of submarine sediment density flows is important, because they transport sediment and organic carbon to the deep sea (Galy et al. 2007), pose a potential hazard to seafloor infrastructure (Chi et al. 2012), and their deposits represent some of the most important hydrocarbon reservoirs on Earth (Stow and Johansson 2000). Determining how such flows behave is key to determining how and where they transport sediment, accurately assessing the threat posed to seafloor structures, and determining the quality of hydrocarbon reservoirs

formed by their deposits (Bruschi et al. 2006; Zakeri et al. 2008; Haughton et al. 2009; Sumner et al. 2009; Baas et al. 2011).

Research over the past 15 years has revealed that sediment density flows may switch between turbulent and laminar regimes and that this “transformation” can strongly affect the geometry and nature of the resultant deposits, as well as the flow itself (Haughton et al. 2009; Talling et al. 2013). In this paper we recognize that turbidity currents and debris flows are two end-member states of the spectrum of submarine, gravity-driven sediment density currents. We define turbidity currents as dilute, typically Newtonian flows in which fluid turbulence is the main particle support mechanism (Mulder and Alexander 2001), and deposit sediment in a layer-by-layer fashion (Talling et al. 2004). Debris flows are typically laminar and cohesive (Kuenen 1951; Hampton 1975; Lowe 1988; Talling et al. 2012; Hermidas et al. 2018). The main particle support mechanisms in debris flows include yield strength, pore pressure, particle buoyancy, and grain-to-grain interactions (Talling et al. 2012). Hybrid flows occur when turbidity currents transform into debris flows (or vice versa). Turbidity currents transform when there is sufficient cohesive sediment available to damp turbulence and transform the flow into a debris flow (Haughton et al. 2003; Talling et al. 2004; Sumner et al. 2009; Baas et al. 2011). The overall flow event (turbidity current and debris flow) is referred to as a hybrid flow. The resulting deposit, which comprises a turbidite juxtaposed with a debrite that is “genetically linked” (i.e., a linked debrite; Haughton et al. 2003; Jackson and Johnson 2009; Talling 2013) is called a hybrid deposit. The incorporation of cohesive sediment into flows has been shown to be an important control on flow rheology, governing when and where flows transform (Sumner et al. 2009; Baas et al. 2011). For instance, a flow may begin as a fully turbulent turbidity current, but through the incorporation of even relatively small amounts (< 1% vol.) of additional cohesive sediment, turbulence can become damped, leading to transformation into a debris flow (Fisher 1983; Sumner et al. 2009; Haughton et al. 2009; Baas et al. 2011; Talling 2013; Patacci et al. 2014). Despite the important role that cohesive sediment plays in the behavior and transformation of sediment density currents, the mechanisms by which mud (and thus clay) is incorporated into and mixed within such flows remain poorly constrained.

One mechanism proposed for the incorporation of cohesive sediments is the direct entrainment of fluid muds from the seafloor. These unconsolidated muds typify much of the global ocean floor (Kineke et al. 1996) and are easily remobilized by sediment density currents (Schieber et al. 2010), readily becoming mixed throughout the flow (Kranenburg and Winterwerp 1997). However, the presence of more consolidated mud clasts, which are often found in sediment-density-current deposits (e.g., Southern et al. 2015), indicates that ingestion and mixing of fluid mud is not the only mechanism to incorporate clay into a flow. Mud clasts may originate from matrix disintegration (i.e., during the early stages of a landslide; Stevenson et al. 2018), or may be plucked from the seafloor by an erosional flow (i.e., rip-up clasts; Patacci et al. 2014; Fonnesu et al. 2016). Mud clasts are also known as mud balls (Bell 1940), clay pebbles (Nossin 1961), clay galls (Pettijohn 1957), intraformational clasts (Smith 1972; Mueller et al. 2017), till balls (Goldschmidt 1994), intraclasts (Chang and Grimm 1999), and mud lumps (Pantin 1967). Once incorporated into a flow, mud clasts are subsequently abraded as they are rolled

along the bed by the density current, resulting in the release of clays into the flow (Bell 1940; Smith 1972), which can cause flow transformation (Sumner et al. 2009; Haughton et al. 2009; Baas et al. 2011). Mud clasts in subaerial environments typically travel between several hundred meters and a few kilometers (Bell 1940; Smith 1972). This contrasts with observations of mud clasts in deep-water deposits that are inferred to have traveled over tens of kilometers or more, although their actual transport distances are often unclear (Table 1). This may be a function of differences between marine and fluvial environments, including the nature of the material in the rip-up clasts, e.g., dry versus saturated clays. We thus limit comparisons with fluvial environments and concentrate on marine environments. Several factors affect how far a mud clast may travel, including initial clast water content (Smith 1972; Mather et al. 2008; Schieber et al. 2010), bed composition (Hermidas et al. 2018), initial size (Smith 1972), clast hardness (Schieber 2016; Stevenson et al. 2018), the presence of extracellular-polymeric substances (EPS; Malarkey et al. 2015), and clast armoring (Bell 1940; Smith 1972).

Mud-Clast Armoring

Mud-clast armoring is observed in many modern environments, including river channels (Bell 1940; Little 1982; Mather et al. 2008), lakes (Dickas and Lunking 1968), coastal environments (Stanley 1969; Tanner 1996), continental shelves (Goldschmidt 1994), submarine channels (Stevenson et al. 2018), and even city streets following heavy rain (Ojakangas and Thompson 1977). The armor is composed of sand and/or gravels that adhere to the soft outer surface of the mud clast as it rolls along the substrate (Bell 1940; Chun et al. 2002). Armor tends to be one grain in thickness (Bell 1940), but it can penetrate a mud clast by up to three grain thicknesses (Chun et al. 2002).

Importantly, the armor is considered to form a permanent protective layer in ephemeral fluvial environments (Bell 1940). Armored mud clasts have been observed in a number of deep marine settings (Table 1). Despite the number of studies citing the presence of armored clasts, the number of studies that cite the presence of mud clasts that are not armored is much greater. As with clast transport generally, armor development may depend on factors such as the stickiness (i.e., initial water content (Smith 1972) and the presence of EPS (Malarkey et al. 2015)), the size of the clast relative to the surrounding sediment (Bell 1940), and clast hardness (Schieber et al. 2010, 2016). Previous experiments have examined the abrasion of air-dried mud chips, simulating clasts sourced from subaerial desiccated mud (Smith 1972), sand-size lithified mudstone (Schieber et al. 2016), and submillimeter- to centimeter-size water-rich kaolinite rip-up fragments (Schieber et al. 2010). However, in the submarine environment, landslides can consist of a variety of sediments (Stevenson et al. 2018) at various stages of consolidation (i.e., a range of shear strengths; Fig. 1). Previous studies have tested the transportation distance of muds at either end of the shear-strength scale—lithified mud (Schieber et al. 2016) as well as mud with a high water content (Schieber et al. 2010). However, no studies have tested the transport-survival prospects of a mud or clay clast of intermediate shear strength (simulating a clast sourced from 1–2 m burial depth; Fig. 1), nor has any previous study tested armoring under controlled conditions. It is also often unclear how far clasts in outcrops have traveled (Table 1). The mechanisms responsible for the development of the armor, the importance of the armor for moderating

clast abrasion rates, and thus the role that armored mud clasts play in the transformation of turbidity currents are poorly understood.

Aims of This Study

We seek to understand how non-lithified clay clasts abrade in a sand-rich turbulent flow and the importance of armoring in modulating the abrasion of mud clasts. First, we aim to understand the mechanism(s) by which mud clasts become armored and whether that armoring is permanent. Second, we determine how armoring affects clast abrasion, and quantify the distance that clasts with and without armor may be transported. As part of this aim, we specifically investigate how varying suspended-sediment concentration and angularity of the sediment in the flow may control clast abrasion. Finally, we consider the implications of clast armoring for flow transformation and the interpretation of deep-water deposits.

METHODS

Our experiments were conducted in a recirculating, ring-shaped annular flume with rotating paddles and a counter rotating base. The annular flume has a radius of 0.53 m, the paddles are 10 cm long, and the channel is 0.23 m deep to the base of the paddles and is 0.145 m wide (Fig. 2A, B). The flume has a total capacity of 160 liters, in which we used fresh water (Fig. 2A, B). The Perspex floor of the annular flume was lined with D₅₀ 158 μm angular Silverbond® sand (by gluing). Secondary circulation was minimized by rotating the base of the tank in the direction opposite to that of the paddles (Sumner et al. 2009). Secondary circulation was considered to be minimized when there was an even deposit of sediment across the width of the channel. Annular flumes have been used in previous studies to simulate long-duration flows (e.g., Smith 1972), and can generate flows with velocities and bed shear stresses comparable to those of natural turbidity currents (Kuenen 1966; Sumner et al. 2008) and as a result can suspend sediment of a size similar to that of sediment found in natural deposits. We test the effect that different flow and sediment parameters have on clast abrasion, specifically: flow velocity, sediment angularity, and suspended-sediment concentration.

Clay Clasts

Each experiment included ten cube-shaped clasts (8 cm³) made of SCOLA air-drying modeling clay. Measurements made by a fall-cone penetrometer show that the clay clasts have undrained shear strengths of 17–40 kPa. These measurements are comparable to normally to lightly overconsolidated sediments found at and close (within 1–2 m depth) to the seafloor at a range of deep-sea sites worldwide (Fig. 1; e.g., Baltzer et al. 1994; Meadows and Meadows 1994; Kuo and Bolton 2013; Yin et al. 2016). Shear strength of the SCOLA clay was not degraded when clasts were remolded. SCOLA clay is composed of quartz (35%), illite smectite (39%), kaolinite (21%), and hematite (5%) (Yin et al. 2016). It is unclear how the stickiness of SCOLA clay would compare with a natural mud, which depends on the clay mineral, clay fraction, plasticity, moisture content, degree of consolidation, as well as shear strength (Kooistra et al. 1998). Therein lies a spectrum of natural variability, which would greatly affect the armoring mechanism being studied here. However, the advantage of using SCOLA clay over a naturally occurring mud is that the properties of the clay are reproducible (i.e., both in these experiments and in further experiments).

Flow Conditions

In the experiments two flow velocities were simulated, 0.5 and 0.7 ms⁻¹, which were found to be the approximate thresholds for sliding and rolling (respectively) of the clasts on a smooth flume floor. The flow velocities used in our experiments produce similar shear stresses ($u^* > 0.09 \text{ ms}^{-1}$) to those of natural sediment gravity flows (Straub and Mohrig 2008; Cartigny et al. 2013; Fig. 2D) (Straub and Mohrig 2008; Cartigny et al. 2013; Fig. 2D). Shear velocity is estimated using

$$U^* = U_{max} k \left[\ln \left(\frac{h_{max}}{0.1 D_{90}} \right) \right]^{-1} \quad (1)$$

Where k is the von Kármán constant (0.4). We assume a logarithmic velocity profile between the bed and the velocity maximum (Van Rijn 1993). We used two sediment types with different angularities: rounded (75–250 μm ballotini), and angular (125–250 μm Silverbond® sand). Runs with bulk sediment concentrations of 0%, 1%, and 10% were performed. However, due to the carrying capacity of the flows, not all of the sediment became suspended. An aggraded bed of up to 1 cm was observed during the 1% bulk sediment experiments, which represents approximately 20% of the sediment added to the flume. A sediment wave the length of the flume of 1 cm to 7 cm height was observed during the 10% bulk sediment experiments, which represents approximately 50% of the sediment added to the flume. Flow profiles were measured using a 1 MHz ultrasonic velocity profiler (UVP) (Fig. 2D). Flow measurements were conducted in independent experimental runs, without the addition of clay clasts, to avoid interaction between the clasts and the UVP probe. In these independent runs, the UVP probe was fixed at 160 mm above the bed and set at an incidence angle of 60° normal to the flow (De Leeuw et al. 2016) with a sediment concentration of 1% angular sand. The velocity was averaged over five minutes. In order to calculate clast travel distance, we use video evidence to determine particle velocity by timing particle movements between vertical pillars on the flume tank. The particle velocity was approximately 85% of the maximum fluid velocity. This value is higher than some previously published values, as the counter-rotating annular flume produces a velocity maximum that is only 7 cm from the bed (Fig. 2).

Experimental Procedure

Experiments were run for one hour. Ten clasts were used in each experiment to provide multiple data points per experiment. Preliminary experiments demonstrated that there was no difference in the rate and type of abrasion with one clast, or ten clasts in the flow. The clasts were cut to size using a cheese wire, and their size was measured using calipers. The clasts were then placed at regular spatial intervals around the channel of the flume tank. Each experiment was conducted at either the slow or fast velocity (0.5 or 0.7 ms⁻¹, respectively). Every ten minutes, the flow was stopped and the clay clasts were retrieved and weighed, photographed, and returned to the flume at regular spatial intervals. After one hour the clay clasts were removed and allowed to dry. During experiments that included suspended sediment, the sediment was allowed to settle out at the end of the ten-minute sample period, and the clasts were put back in on top of the bed. A subsample of angular sediment was removed from the armor of two clasts for analysis using a Hitachi TIM-1000 scanning electron microscope (SEM).

RESULTS

Armoring Mechanisms

Clasts became more rounded and smaller as the experiments progressed (Figs. 3, 4). In experiments with sediment, clasts became armored within the first ten minutes of the experiment as they rolled along the substrate (Fig. 5). These clasts then transitioned through four morphological stages as they abraded (Figs. 4, 6). In stage 1, the cube-shaped clasts were observed to roll or bounce along the bed. When the clasts were removed after ten minutes, they had become either barrel shaped (stage 2) or subrounded (stage 3). During stage 2, the clasts were barrel shaped and armored only along the minor axis, and not the barrel tops and bottoms, which were also softer than the rest of the clast. Stage 2 was observed only in the 10%-sediment-concentration experiments, and was probably not observed in other experiments due to this stage being shorter than the ten-minute measurement period. In stage 3, the clasts became subrounded (but not fully spherical) and armored around all axes; the softened tops and bottoms of the barrel shaped clasts had abraded. In stage 4, the clasts were both rounded and armored. The clasts continued to abrade, and the rate of abrasion declined with decreasing size and increasing sphericity. The latter two stages occupied 57–85% of each experiment. In all experiments except the 10%-concentration experiments, the clasts had reached stage 4 by the end of the one-hour experiment. The exceptions to this were the 10% angular sand experiments, in which clasts abraded the slowest and had attained only stage 3 by the end of the experiment. SEM images of sand grains that fell out of armored clasts show that the sand grains have clay particles attached to them (Fig. 6).

Clast Travel Distance

Complete clast disintegration occurred in some, but not all experimental runs by the end of the one-hour measurement period (Fig. 7A, B). When normalized to weight and travel distance, the shape of the disintegration curves were found to be similar for most of the experiments, with the exception of experiments using 10% bulk angular sand (Fig. 7C). Experiments using 10% angular sand display a shallower normalized curve than the other experiments.

Clasts abraded most quickly in clear-water experiments, where they were gradually but completely destroyed over projected distances of < 2 km. Clay clasts developed armor following the addition of sand to the experiments. The development of armor coincided with a reduction in the rate of abrasion whereby armored clasts traveled at least twice as far as unarmored clasts. Abrasion was further reduced by decreasing flow velocity, increasing sediment concentration, and by using angular sand grains (rather than rounded sand grains). At the lowest velocity (0.5 ms^{-1}), at the highest sediment concentration (10%), and by using angular sand grains in the experiment, the clasts traveled almost four times farther than unarmored clasts (Fig. 7).

DISCUSSION

The experiments show that clay clasts passed through four stages as they abraded: 1) cube-shaped, 2) barrel-shaped, 3) subrounded, and 4) rounded (Figs. 4, 6). Abrasion rate is controlled by flow velocity, bed hardness, and to a lesser extent the angularity of the armoring sand at lower flow velocities. Abrasion was slower and clasts passed through the four stages more slowly when velocity was lower, there was a thicker aggraded sand

bed (softer substrate), and angular rather than rounded sediment was used in the experiment. In experiments that included sediment, clasts developed a layer of armor that was one grain thick (Figs. 3, 5). Unarmored mud clasts were abraded by a combination of impacting the bed (Bell 1940; Smith 1972), and wetting of the clast surface, reducing its shear strength (Smith 1972), leading to increased likelihood of abrasion or dilution. We infer that an armored mud clast would still be able to lose volume via the wetting and abrasion, and the wetting and dilution methods described above, but this would occur only between armor grains, and thus at a lower rate for an unarmored clast. The wetted clay between the armor grains would be extruded and eroded or diluted. In addition, clay is plucked from the clasts as the sand armor falls away and is subsequently replenished; this is evidenced by the presence of clays on the sand armor in SEM images (Fig. 6). Thus, we show that armoring increases the distance that clasts can be transported over a hard flume floor before they are destroyed, by up to several kilometers. We now discuss the process of mud-clast armoring and the transient nature of the armor observed during the experiments.

Armoring Mechanisms

Here we document that armoring occurs via rolling of cohesive clasts along a sandy substrate. During Stage 2 (barrel shape) of clast evolution the clasts were armored around the exterior of the barrel, but the barrel tops and bottoms were soft and unarmored. This indicates that the clasts roll along a preferential axis when not rounded, and that the clasts develop armor only on surfaces that come into contact with the substrate, rather than developing an armor via bombardment with sand grains from suspension. A naturally occurring unarmored clast of a shear strength similar to that of our clasts may indicate a lack of rolling (i.e., suspension or matrix transport) or rolling along a non-granular bed (e.g., mud).

Our results oppose previous suggestions in fluvial environments that armoring is permanent, that falls away only as clasts become dry, and that armored clasts abrade only as they impact upon boulders (Bell 1940). We find that the armor is semipermanent, that clay is extruded and eroded or diluted, and that the individual grains that make up the armor are removed and replenished and remove particles of clay as they do so. We infer the armoring and abrasion mechanism from the presence of clay on the sand particles in SEM images, and from the fact that the clasts are always covered in sand when extracted for measuring yet they decrease in size through time. Therefore, in order to be maintained, the armor must be replenished from a granular substrate. The armoring process is therefore transient, and more dynamic than previously considered.

Armoring and Mud-Clast Travel Distances

We now consider why some mud clasts in natural systems appear to travel farther than those in our experiments, as illustrated by the potentially long-runout Grand Banks turbidity current that occurred in 1929, offshore Newfoundland.

The inferred travel distance of the armored mud clasts in the 1929 Grand Banks turbidity current is two orders of magnitude greater (> 400 km) than the findings of our experiments (2–12 km). Here we seek an explanation for this apparent discrepancy.

First, we consider the size of the mud clasts in the 1929 Grand Banks event compared to our laboratory experiment. The Grand Banks event transported > 150 km³ of sediment

(Piper and Aksu 1987) in a series of submarine landslides with shear planes of 5–25 m depth (Piper et al. 1999). It is probable that some of the blocks were meters in size, which may have facilitated their long transport distance. However, if we compare our clear-water experiment with a similar experiment by Smith et al. (1972) that used larger clasts, we see that clast abrasion rates are much higher for larger clasts (Fig. 8). Therefore, whilst initial clasts size must have some effect on the distance that a clast can travel, it may not be as important as it first seems.

Second, we consider the shear strength of the mud clasts in the 1929 Grand Banks event compared to the clasts in our experiments. The initial water content (Smith 1972) and the hardness of clasts (Lewin and Brewer 2002) are important when considering abrasion rates. There are no known shear-strength measurements of clasts in the Grand Banks deposit, but near-seafloor muds around the Grand Banks region and offshore Nova Scotia have been shown to be overconsolidated (Clark and Landva 1988; Baltzer et al. 1994). The Grand Banks shelf is a glacially modified margin (Piper et al. 1999), thus explaining the presence of highly consolidated seafloor muds due to past glacial loading. Other locations around the world also feature overconsolidated sediments, with an extreme example noted on the UK Continental Shelf where ice loading during the last glaciation has resulted in near-seafloor (< 5 m) undrained shear strengths in excess of 2500 kPa (Aldridge and Carrington 2010). In addition, the shear plane of the Grand Banks landslide was 5–25 m deep (Piper et al. 1999), which is within the region of the overconsolidated muds found on the UK Continental Shelf (Aldridge and Carrington 2010). The shear strength of the clasts produced during landslide disintegration may therefore have been greater than the shear strength of the clasts used in our experiments (17–40 kPa). Experimental studies have shown that higher-shear-strength substrates will resist erosion more than lower-strength ones (Winterwerp et al. 1992, 2012; Schieber et al. 2010; Schieber 2016). In the same manner, higher shear strengths may therefore improve the durability of mud clasts and facilitate a longer transport distance of the clasts, as inferred from the Grand Banks deposit.

Fourth, we consider the mode of transport of the mud clasts in the 1929 Grand Banks event compared to our laboratory experiments. Field evidence suggests that rolling along the bed, rather than being in suspension, is important for promoting clast abrasion (Bell 1940; Schwab et al. 1996; Talling et al. 2010). Clasts can travel hundreds of kilometers if they are encased in a debris flow (Schwab et al. 1996; Talling et al. 2010). Two mud clasts were found in cores of the Grand Banks deposit, and both of them were armored (Stevenson et al. 2018), indicating rolling along a sand-rich bed. The extreme travel distance of clasts in the Grand Banks density current can be explained by the downslope evolution of the density current. The density current began as a debris flow, and remained as such for the first 20–35 km of transport (Piper et al. 1999). Clasts in the flow at this stage would likely not have been armored, but would have been protected by the surrounding debris flow. After the debris flow phase, the density current then transformed on steep slopes into a turbidity current (Piper et al. 1999). The turbidity current was shown to have attained a velocity of up to 19 ms^{-1} (Piper et al. 1999). Such a high velocity is likely to support mud clasts in suspension, which would mean that they were not rolling during the high-velocity section of the journey. The clasts may have been fully

suspended in the high-velocity flow. As the flow began to lose energy and decelerate on the more distal slopes, the clasts would have fallen out of suspension and rolled along the bed. In addition to the sequence of events, the average bulk sediment concentration of the Grand Banks density current is estimated to have been 2.7–5.5% (Stevenson et al. 2018). In our experiments we found a flow-averaged concentration of 1% to be suitable in supplying the clasts with sediment to replace dislodged armor particles. The combination of the transforming, fast flow, together with the high average sediment concentration, probably enabled the mud clasts in the Grand Banks density current to attain their impressive transport distances.

Finally, we consider the nature of the substrate over which the clasts were carried (assuming that they were not necessarily in suspension) as our experiments suggest that bed hardness may affect transport distance. In real-world systems, such as the Grand Banks, the strength of the seafloor substrate is likely to vary and, in places (e.g., where it is muddy), may be considerably softer than the floor of our flume.

To summarize the Grand Banks case study: it is probable that the long travel distances can be explained by the large initial size and high shear strength of the clasts, and the soft nature of the seafloor substrate over which the flow traveled. Furthermore, it is possible that, given the velocity attained by the flow, the clasts were suspended for at least part of their journey, thus reducing their abrasion. It is likely that a combination of these factors resulted in the unusually long transport distances attained by clasts in the 1929 Grand Banks density current.

The Prevalence of Unarmored Mud Clasts

There are a number of examples of armored mud clasts from deep marine settings, but the examples of unarmored mud clasts greatly outnumber these. Here we consider why this imbalance exists. The imbalance between armored and unarmored clast examples could be due to several reasons. A first reason could be due to the stickiness of the mud; mud clasts that are very wet (e.g., mud with a high fluid content; Schieber et al. 2010) or clasts that are very hard (e.g., lithified or highly overconsolidated mud; Schieber 2016) may not be able to support an armor layer. A second reason for the relatively common occurrence of unarmored mud clasts could be that armor falls away once it can be no longer replenished. As the sediment gravity flow reaches the distal muddy fringes of the turbidite system, it will no longer replenish the armor and may simply lose its armor coating due to wetting and/or dilution effects. Furthermore, clasts transported across a soft (i.e., mud) floor would experience a potentially greatly reduced rate of abrasion (particularly compared to the hard flume floor of this study) and may be transported farther or even increase their mass by accreting additional mud, as well as having more opportunity to shed their armor. Finally, the average grain size of the system may be too fine for armoring to occur; mud clasts can be armored only by grains coarser than silt (Bell 1940); if the system is too muddy, armor will not form.

Implications for Interpreting Clast-Bearing Sediment-Density-Current Deposits

In this section we discuss how armoring of clasts may control where linked debrites develop, and how armored mud clasts may help in identifying linked debrites in outcrop.

Previous studies have identified that turbidity currents commonly transform into debris flows and deposit debrites towards the lateral or distal edges of turbidite systems

(Haughton et al. 2009; Kane and Pontén 2012; Fonnesu et al. 2015, 2016, 2018). However, it can be difficult to determine whether a debrite is part of a hybrid deposit when there is limited outcrop exposure. Distal flow transformation is promoted by the incorporation of clay, which is often associated with disaggregation of mud clasts (Patacci et al. 2014). Armored mud clasts have been found in turbidites (Stanley 1964; Dasgupta and Buatois 2012; Fonnesu et al. 2018), hyperpycnites (Ponce and Carmona 2011), and hybrid deposits (Haughton et al. 2003; Felix et al. 2009; Patacci et al. 2014). The presence of armored mud clasts in a debrite indicates up-dip transformation from a turbidity current to a debris flow, because rolling of the mud clasts along a sandy bed is required in order for the sandy armor to develop (Fig. 9).

Turbidity currents transform into debris flows once a sufficient quantity of cohesive sediment is available in the flow, and once turbulence is low enough for the gelling of clay particles, which typically occurs as the flow decelerates (Baas et al. 2009; Sumner et al. 2009). Our experiments show that armoring reduces the rate of abrasion of mud clasts and thus would reduce the rate of release of clay into a turbidity current. If a sufficient volume of clasts is present, then armoring could hinder the transformation of turbidity currents, and may contribute to hybrid deposits occurring preferentially in lateral and distal parts of turbidite systems (Fig. 9). We find in our experiments that clast armor is transient and requires replenishment from the substrate. Once the clast-bearing flow reaches the distal reaches of the fan it is likely to encounter mud-rich substrates, and clasts will no longer be able to replenish their armor. This may partly explain why unarmored rather than armored clasts are found most often.

CONCLUSIONS

Our first aim was to understand the mechanism(s) by which mud clasts become armored and if that armoring is permanent. We find that clasts go through the same four stages of evolution regardless of the development of an armor layer, but the armor layer reduces the rate of abrasion. We provide the first direct evidence that armoring occurs by rolling clasts in a sandy substrate. We also show for the first time that clast armor is transient and undergoes continual replenishment from the bed. Unarmored clasts may be indicative of a lack of rolling (traveled a short distance, traveled in suspension, or traveled as a floating outside clast in a debris flow, for example), a lack of available sediment that can form armor (i.e., a muddy bed), or that the clay that forms the clast is too hard to support armor.

Our second aim was to determine how armoring affects clast abrasion and to quantify the distance clasts with and without armor can be transported. Without armor on a hard flume floor, 8 cm³ cube-shaped clasts disintegrate within two kilometers. Following the addition of a 1% concentration of suspended sediment, an armor develops around clasts that more than doubles the distance they can travel. We find that the rate of abrasion further declines with increasing sediment concentration, thus increasing travel distance by more than four times the distance achieved by unarmored clasts. A sandy substrate can help to improve the transport distance of a clay clast by providing an armor of sand. However, natural systems can have muddy substrates, which we did not consider in these experiments. Unarmored clasts may travel farther on muddy rather than sandy substrates because the muddy substrate causes less erosion to the clast than a hard substrate.

Additional experiments are required to investigate the transport distances achievable by mud clasts over a muddy substrate, as well as of armored mud clasts over a muddy substrate.

Our final aim was to consider the implications of clast armor for interpreting deep-water deposits and flow transformations. Our results suggest that the presence of armored clasts in debrites may serve as a tool for identifying linked debrites. Our results also suggest that armor may delay flow transformation and be partly responsible for the common occurrence of flow transformation in distal lobe environments at the point that the seabed becomes muddy, and therefore the sand armor can no longer be replenished.

REFERENCES

- Aldridge, T.R., and Carrington, T.M., 2010, BP Clair phase 1-pile driveability and capacity in extremely hard till: *Frontiers in Offshore Geotechnics II, Proceedings*, p. 477–482, doi: 10.1201/b10132-60 10.1201/b10132-60.
- Baas, J.H., Best, J.L., and Peakall, J., 2011, Depositional processes, bedform development and hybrid bed formation in rapidly decelerated cohesive (mud–sand) sediment flows: *Sedimentology*, v. 58, p. 1953–1987, doi: 10.1111/j.1365-3091.2011.01247.x.
- Baltzer, A., Cochonat, P., and Piper, D.J.W., 1994, In situ geotechnical characterization of sediments on the Nova Scotian Slope, eastern Canadian continental margin: *Marine Geology*, v. 120, p. 291–308, doi: 10.1016/0025-3227(94)90063-9.
- Bell, H.S., 1940, Armored mud balls: their origin, properties, and role in sedimentation: *Geology*, v. 48, p. 1–31.
- Bruschi, R., Bughi, S., Spinazzé, M., Torselletti, E., and Vitali, L., 2006, Impact of debris flows and turbidity currents on seafloor structures: *Norsk Geologisk Tidsskrift*, v. 86, p. 317–336.
- Cartigny, M.J.B., Eggenhuisen, J.T., Hansen, E.W.M., and Postma, G., 2013, Concentration-dependent flow stratification in experimental high-density turbidity currents and their relevance to turbidite facies models: *Journal of Sedimentary Research*, v. 83, p. 1046–1064, doi: 10.2110/jsr.2013.71.
- Chang, A.S., and Grimm, K.A., 1999, Speckled beds: distinctive gravity-flow deposits in finely laminated diatomaceous sediments, Miocene Monterey Formation, California: *Journal of Sedimentary Research*, v. 69, p. 122–134, doi: 10.2110/jsr.69.122.
- Chi, K., Zakeri, A., and Hawlader, B., 2012, Impact drag forces on pipelines caused by submarine glide blocks or out-runner blocks, *in* Yamada, Y., Kawamura, K., Ikehara, K., Ogawa, Y., Urgeles, R., Mosher, D., Chaytor, J., and Strasser, M., eds., *Submarine Mass Movements and Their Consequences*: Dordrecht, Springer, p. 429–440, doi: 10.1007/978-94-007-2162-3.
- Chun, S.S., Choe, M.Y., and Chough, S.K., 2002, Armored mudstone boulders in submarine debris-flow deposits, the Hunghae Formation, Pohang Basin: evidence for the large-scale slumping of adjacent area of a submarine channel or scar wall: *Geosciences Journal*, v. 6, p. 215–225, doi: 10.1007/BF02912692.
- Dasgupta, S., and Buatois, L., 2012, Unusual occurrence and stratigraphic significance of the *Glossifungites* Ichnofacies in a submarine paleo-canyon: example from a Pliocene

shelf-edge delta, southeast Trinidad: *Sedimentary Geology*, v. 269–270, p. 69–77, doi: 10.1016/j.sedgeo.2012.06.004.

De Leeuw, J., Eggenhuisen, J.T., and Cartigny, M.J.B., 2016, Morphodynamics of submarine channel inception revealed by new experimental approach: *Nature Communications*, v. 7, p. 1–7, doi: 10.1038/ncomms10886.

Dickas, A.B., and Lunking, W., 1968, The origin and destruction of armored mud balls in a fresh-water lacustrine environment, Lake Superior: *Journal of Sedimentary Petrology*, v. 38, p. 1366–1370, doi: 10.1306/74D71B9F-2B21-11D7-8648000102C1865D.

Ehlers, C.J., Chen, J., Roberts, H.H., and Lee, Y.C., 2005, The origin of near-sea floor cruts zones in deepwater: Perth, 1st International Symposium on Frontiers in Offshore Geotechnics, Proceedings, p. 927–933.

Felix, M., Leszczyński, S., Ślaczka, A., Uchman, A., Amy, L., and Peakall, J., 2009, Field expressions of the transformation of debris flows into turbidity currents, with examples from the Polish Carpathians and the French Maritime Alps: *Marine and Petroleum Geology*, v. 26, p. 2011–2020, doi: 10.1016/j.marpetgeo.2009.02.014.

Fisher, R., 1983, Flow transformations in sediment gravity flows: *Geology*, v. 11, p. 273–274.

Fonnesu, M., Haughton, P., Felletti, F., and McCaffrey, W., 2015, Short length-scale variability of hybrid event beds and its applied significance: *Marine and Petroleum Geology*, v. 67, p. 583–603, doi: 10.1016/j.marpetgeo.2015.03.028.

Fonnesu, M., Patacci, M., Haughton, P.D.W., and Felletti, F., 2016, Hybrid event beds generated by local substrate delamination on a confined basin floor: *Journal of Sedimentary Research*, v. 86, p. 929–943.

Fonnesu, M., Felletti, F., Haughton, P.D.W., Patacci, M., and McCaffrey, W.D., 2018, Hybrid event bed character and distribution linked to turbidite system sub-environments: the North Apennine Gottero Sandstone (north-west Italy): *Sedimentology*, v. 65, p. 151–190, doi: 10.1111/sed.12376.

Galy, V., France-Lanord, C., Beyssac, O., Faure, P., Kudrass, H., and Palhol, F., 2007, Efficient organic carbon burial in the Bengal fan sustained by the Himalayan erosional system: *Nature*, v. 450, p. 407–410.

Goldschmidt, P.M., 1994, Armored and unarmored till balls from the Greenland Sea floor: *Marine Geology*, v. 121, p. 121–128.

Grupe, B., Becker, H.J., and Oebius, H.U., 2001. Geotechnical and sedimentological investigations of deep-sea sediments from a manganese nodule field of the Peru Basin: *Deep Sea Research Part II: Topical Studies in Oceanography*, v. 48, p. 3593–3608.

Gutmacher, C.E., and Normark, W.R., 2002, Sur submarine landslide, a deep-water sediment slope failure, *in* Schwab, W.C., Lee, H.J., and Twichell, D.C., eds., U.S. Geological Survey, Bulletin 2002, p. 158–166.

Hampton, M.A., 1975, Competence of fine-grained debris flows: *Journal of Sedimentary Petrology*, v. 45, p. 834–844.

Haughton, P.D.W., Barker, S.P., and McCaffrey, W.D., 2003, “Linked” debrites in sand-rich turbidite systems: origin and significance: *Sedimentology*, v. 50, p. 459–482, doi: 10.1046/j.1365-3091.2003.00560.x.

Haughton, P., Davis, C., McCaffrey, W., and Barker, S., 2009, Hybrid sediment gravity flow deposits: classification, origin and significance: *Marine and Petroleum Geology*, v. 26, p. 1900–1918, doi: 10.1016/j.marpetgeo.2009.02.012.

Hermidas, N., Eggenhuisen, J.T., Jacinto, R.S., Luthi, S.M., Toth, F., and Pohl, F., 2018, A classification of clay-rich subaqueous density flow structures: *Journal of Geophysical Research*, v. 123, p. 945–966, doi: 10.1002/2017JF004386.

Jackson, C., and Johnson, H.D., 2009, Sustained turbidity currents and their interaction with debris-related topography: Labuan Island, offshore NW Borneo, Malaysia: *Sedimentary Geology*, v. 219, p. 77–96, doi: 10.1016/j.sedgeo.2009.04.008.

Kane, I.A., and Pontén, A.S.M., 2012, Submarine transitional flow deposits in the Paleogene Gulf of Mexico: *Geology*, v. 40, p. 1119–1122, doi: 10.1130/G33410.1.

Kineke, G.C., Sternberg, R.W., Trowbridge, J.H., and Geyer, W.R., 1996, Fluid-mud processes on the Amazon continental shelf: *Continental Shelf Research*, v. 16, p. 667–696, doi: 10.1016/0278-4343(95)00050-X.

Kooistra, A., Verhoef, P.N.W., Broere, W., Ngan-Tillard, D.J.M., and van Tol, A.N., 1998, Appraisal of stickiness of natural clays from laboratory tests: of the 25 Years Delft, Jubilee Symposium of Engineering Geology in the Netherlands, *Proceedings*, 101–113 p.

Kranenburg, C., and Winterwerp, J.C., 1997, Erosion of fluid mud layers: *Journal of Hydraulic Engineering*, v. 123, p. 504–511, doi: 10.1061/(ASCE)0733-9429(1997)123:6(512).

Kuenen, H., 1951, Properties of turbidity currents of high density, *in* Hough, J.L., ed., *Turbidity Currents and the Transportation of Coarse Sediments to Deep Water*: Society of Economic Paleontologists and Mineralogists, Special Publication 2, p. 14–33.

Kuenen, H., 1966, Experimental turbidite lamination in a circular flume: *The Journal of Geology*, v. 74, p. 523–545.

Kuo, M., and Bolton, M., 2013, The nature and origin of deep ocean clay crust from the Gulf of Guinea: *Géotechnique*, v. 63, p. 500–509, doi: 10.1680/geot.10.P.012.

Lewin, J., and Brewer, P.A., 2002, Laboratory simulation of clast abrasion: *Earth Surface Processes and Landforms*, v. 27, p. 145–164, doi: 10.1002/esp.306.

Little, R.D., 1982, Lithified armored mud balls of the Lower Jurassic Turners Falls sandstone, north-central Massachusetts: *Geology*, v. 90, p. 203–207.

Lowe, D.R., 1988, Suspended load fallout rate as an independent variable in the analysis of current structures: *Sedimentology*, v. 35, p. 765–776, doi: 10.1111/j.1365-3091.1988.tb01250.x.

Malarkey, J., Baas, J.H., Hope, J.A., Aspden, R.J., Parsons, D.R., Peakall, J., Paterson, D.M., Schindler, R.J., Ye, L., Lichtman, I.D., Bass, S.J., Davies, A.G., Manning, A.J., and Thorne, P.D., 2015, The pervasive role of biological cohesion in bedform development: *Nature Communications*, v. 6, p. 1–6, doi: 10.1038/ncomms7257.

Mather, A., Stokes, M., Pirrie, D., and Hartley, R., 2008, Generation, transport and preservation of armored mudballs in an ephemeral gully system: *Geomorphology*, v. 100, p. 104–119, doi: 10.1016/j.geomorph.2007.10.030.

Meadows, A., and Meadows, P.S., 1994, Bioturbation in deep sea Pacific sediments: *Geological Society of London, Journal*, v. 151, p. 361–375, doi: 10.1144/gsjgs.151.2.0361.

- Mueller, P., Patacci, M., and Di Giulio, A., 2017, Hybrid event beds in the proximal to distal extensive lobe domain of the coarse-grained and sand-rich Bordighera turbidite system (NW Italy): *Marine and Petroleum Geology*, v. 86, p. 908–931, doi: 10.1016/j.marpetgeo.2017.06.047.
- Nossin, J.J., 1961, Occurrence and origin of clay pebbles on the East Coast of Johore, Malaya: *Journal of Sedimentary Petrology*, v. 31, p. 437–447, doi: 10.1306/74D70B91-2B21-11D7-8648000102C1865D.
- Ojakangas, R.W., and Thompson, J.A., 1977, Modern armored mud balls in an urban environment: *Journal of Sedimentary Petrology*, v. 47, p. 1630–1633.
- Pantin, H.M., 1967, The origin of water-borne diamictites and their relation to turbidites: *New Zealand Journal of Marine and Freshwater Research*, v. 1, p. 118–138, doi: 10.1080/00288330.1967.9515198.
- Patacci, M., Haughton, P.D.W., and McCaffrey, W.D., 2014, Rheological complexity in sediment gravity flows forced to decelerate against a confining slope, Braux, SE France: *Journal of Sedimentary Research*, v. 84, p. 270–277.
- Pettijohn, F.J., 1957, *Sedimentary Rocks*: New York, Harper and Brothers, 718 p.
- Piper, D.J.W., and Aksu, A.E., 1987, The source and origin of the 1929 Grand Banks turbidity current inferred from sediment budgets: *Geo-Marine Letters*, v. 7, p. 177–182, doi: 10.1007/BF02242769.
- Piper, D.J.W., Cochonat, P., and Morrison, M.L., 1999, The sequence of events around the epicenter of the 1929 Grand Banks earthquake: initiation of debris flows and turbidity currents inferred from sidescan sonar: *Sedimentology*, v. 46, p. 79–97.
- Ponce, J.J., and Carmona, N., 2011, Coarse-grained sediment waves in hyperpycnal clinof orm systems, Miocene of the Austral foreland basin, Argentina: *Geology*, v. 39, p. 763–766, doi: 10.1130/G31939.1.
- Schieber, J., 2016, Experimental testing of the transport-durability of shale lithics and its implications for interpreting the rock record: *Sedimentary Geology*, v. 331, p. 162–169, doi: 10.1016/j.sedgeo.2015.11.006.
- Schieber, J., Southard, J.B., and Schimmelmann, A., 2010, Lenticular shale fabrics resulting from intermittent erosion of water-rich muds: interpreting the rock record in the light of recent flume experiments: *Journal of Sedimentary Research*, v. 80, p. 119–128, doi: 10.2110/jsr.2010.005.
- Schwab, W.C., Lee, H.J., Twichell, D.C., Locat, J., Nelson, C.H., McArthur, W.G., and Kenyon, N.H., 1996, Sediment mass-flow processes on a depositional lobe, outer Mississippi Fan: *Journal of Sedimentary Research*, v. 66, p. 916–927, doi: 10.1306/D426843C-2B26-11D7-8648000102C1865D.
- Smith, N.D., 1972, Flume experiments on the durability of mud clasts: *Journal of Sedimentary Petrology*, v. 42, p. 378–383, doi: 10.1306/74D72559-2B21-11D7-8648000102C1865D.
- Southern, S.J., Patacci, M., Felletti, F., and McCaffrey, W.D., 2015, Influence of flow containment and substrate entrainment upon sandy hybrid event beds containing a co-genetic mud-clast-rich division: *Sedimentary Geology*, v. 321, p. 105–122.
- Stanley, D.J., 1964, Large mudstone-nucleus sandstone spheroids in submarine channel deposits: *Journal of Sedimentary Petrology*, v. 34, p. 672–676.

Stanley, D.J., 1969, Armored mud balls in an intertidal environment, Minas Basin, southeast Canada: *Geology*, v. 77, p. 683–693.

Stevenson, C.J., Talling, P.J., Sumner, E.J., Masson, D.G., Frenz, M., and Wynn, R.B., 2014, On how thin submarine flows transported large volumes of sand for hundreds of kilometres across a flat basin plain without eroding the sea floor: *Sedimentology*, v. 61, p. 1982–2019.

Stevenson, C.J., Feldens, P., Georgiopoulou, A., Sch□nke, M., Krastel, S., Piper, D.J.W., Lindhorst, K., and Mosher, D., 2018, Reconstructing the sediment concentration of a giant submarine gravity flow: *Nature Communications*, v. 9, p. 2616, doi: 10.1038/s41467-018-05042-6.

Stow, D.A.V., and Johansson, M., 2000, Deep-water massive sands: nature, origin and hydrocarbon implications: *Marine and Petroleum Geology*, v. 17, p. 145–174, doi: 10.1016/S0264-8172(99)00051-3.

Straub, K.M., and Mohrig, D., 2008, Quantifying the morphology and growth of levees in aggrading submarine channels: *Journal of Geophysical Research: Earth Surface*, v. 113, p. 1–20, doi: 10.1029/2007JF000896.

Sumner, E.J., Amy, L.A., and Talling, P.J., 2008, Deposit structure and processes of sand deposition from a decelerating sediment suspension: *Journal of Sedimentary Research*, v. 78, p. 529–547, doi: 10.2110/jsr.2008.062.

Sumner, E.J., Talling, P.J., and Amy, L.A., 2009, Deposits of flows transitional between turbidity current and debris flow: *Geology*, v. 37, p. 991–994, doi: 10.1130/G30059A.1.

Sumner, E.J., Talling, P.J., Amy, L.A., Wynn, R.B., Stevenson, C.J., and Frenz, M., 2012, Facies architecture of individual basin-plain turbidites: comparison with existing models and implications for flow processes: *Sedimentology*, v. 59, p. 1850–1887.

Sylvester, Z., and Lowe, D., 2004, Textural trends in turbidites and slurry beds from the Oligocene flysch of the East Carpathians, Romania: *Sedimentology*, v. 51, p. 945–972.

Talling, P.J., 2013, Hybrid submarine flows comprising turbidity current and cohesive debris flow: deposits, theoretical and experimental analyses, and generalized models: *Geosphere*, v. 9, p. 460–488, doi: 10.1130/GES00793.1.

Talling, P.J., Amy, L.A., Wynn, R.B., Peakall, J., and Robinson, M., 2004, Beds comprising debrite sandwiched within co-genetic turbidite: origin and widespread occurrence in distal depositional environments: *Sedimentology*, v. 51, p. 163–194, doi: 10.1111/j.1365-3091.2004.00617.x.

Talling, P.J., Wynn, R.B., Schmidt, D.N., Rixon, R., Sumner, E., and Amy, L., 2010, How did thin submarine debris flows carry boulder-sized intraclasts for remarkable distances across low gradients to the far reaches of the Mississippi Fan?: *Journal of Sedimentary Research*, v. 80, p. 829–851, doi: 10.2110/jsr.2010.076.

Talling, P.J., Masson, D.G., Sumner, E.J., and Malgesini, G., 2012, Subaqueous sediment density flows: depositional processes and deposit types: *Sedimentology*, v. 59, p. 1937–2003, doi: 10.1111/j.1365-3091.2012.01353.x.

Tanner, L.H., 1996, Armored mud balls revisited: *Atlantic Geology*, v. 32, p. 123–125.

Van Rijn, L.C., 1993, *Principles of sediment transport in rivers, estuaries, and coastal seas*, Aqua Publications, 790 p.

Winterwerp, J.C., Bakker, W.T., Mastbergen, D.R., and Van Rossum, H., 1992, Hyperconcentrated sand–water mixture flows over an erodible bed: *Journal of Hydraulic Engineering*, v. 118, p. 1508–1525.

Winterwerp, J.C., Van Kesteren, W.G.M., Van Prooijen, B.C., and Jacobs, W., 2012, A conceptual framework for shear flow-induced erosion of soft cohesive sediment beds: *Journal of Geophysical Research*, v. 117, p. C10020, doi: 10.1029/2012JC008072.

Yin, D., Peakall, J., Parsons, D., Chen, Z., Averill, H.M., Wignall, P., and Best, J., 2016, Bedform genesis in bedrock substrates: insights into formative processes from a new experimental approach and the importance of suspension-dominated abrasion: *Geomorphology*, v. 255, p. 26–38, doi: 10.1016/j.geomorph.2015.12.008.

Zakeri, A., Hoeg, K., Nadim, F., Uio, O., and Centre, I., 2008, OTC 19173 Submarine debris flow impact on pipelines: drag forces, mitigation, and control: *Offshore Technology Conference, Proceedings*.

Received 23 January 2019; accepted 9 March 2020.

FIGURE CAPTIONS

FIG. 1.—The range in undrained-shear-strength profiles of various seafloor muds from around the globe.

FIG. 2.—Experimental setup showing **A**) cross-sectional view of the annular flume with dimensions, **B**) a plan view of the annular flume, **C**) the orientation of the UVP in the annular flume, **D**) the velocity profile recorded by the UVP for the fast (gray dash) and slow (black) flume settings.

FIG. 3.—Clasts at various stages of their evolution.

FIG. 4.—The average shape and length of the longest axis of the clasts through time. Red numbers indicate fast ($\sim 0.7 \text{ ms}^{-1}$) flow averages, and black numbers indicate slow ($\sim 0.5 \text{ ms}^{-1}$) flow averages.

FIG. 5.—**A**) A close-up photograph of an armored clast. **B**) A close-up photograph of an unarmored clast.

FIG. 6.—Scanning-electron-microscope images of angular sediment grain samples. **A–B**) Examples of angular sediment before the experiment, **C–D**) examples of angular sediment taken from the periphery of an armored clast. The grains clearly show clay that has adhered to the surface of the grains.

FIG. 7.—**A**) The average length of the longest axis plotted against travel distance. **B**) Normalized average showing original clast weight plotted against travel distance. Error bars show the range of measurements. **C**) Normalized distance versus normalized weight showing that abrasion rates are broadly similar. **D**) The extrapolated distance the clasts would travel until they are destroyed by the flow. Extrapolated using an exponential function; $\exp(-a*x+b)$. The dashed gray line indicates the last point at which clasts were recovered in the 0.7 ms^{-1} clear-water experiment, and is used as an approximate travel distance.

FIG. 8.—Comparison between the abrasion rate of clasts in clear-water experiments of Smith (1972) and the clear-water experiments presented here. The clasts in the Smith (1972) experiment were $3 \text{ cm} \times 0.5 \text{ cm}$ whereas our clasts were 2 cm cuboids.

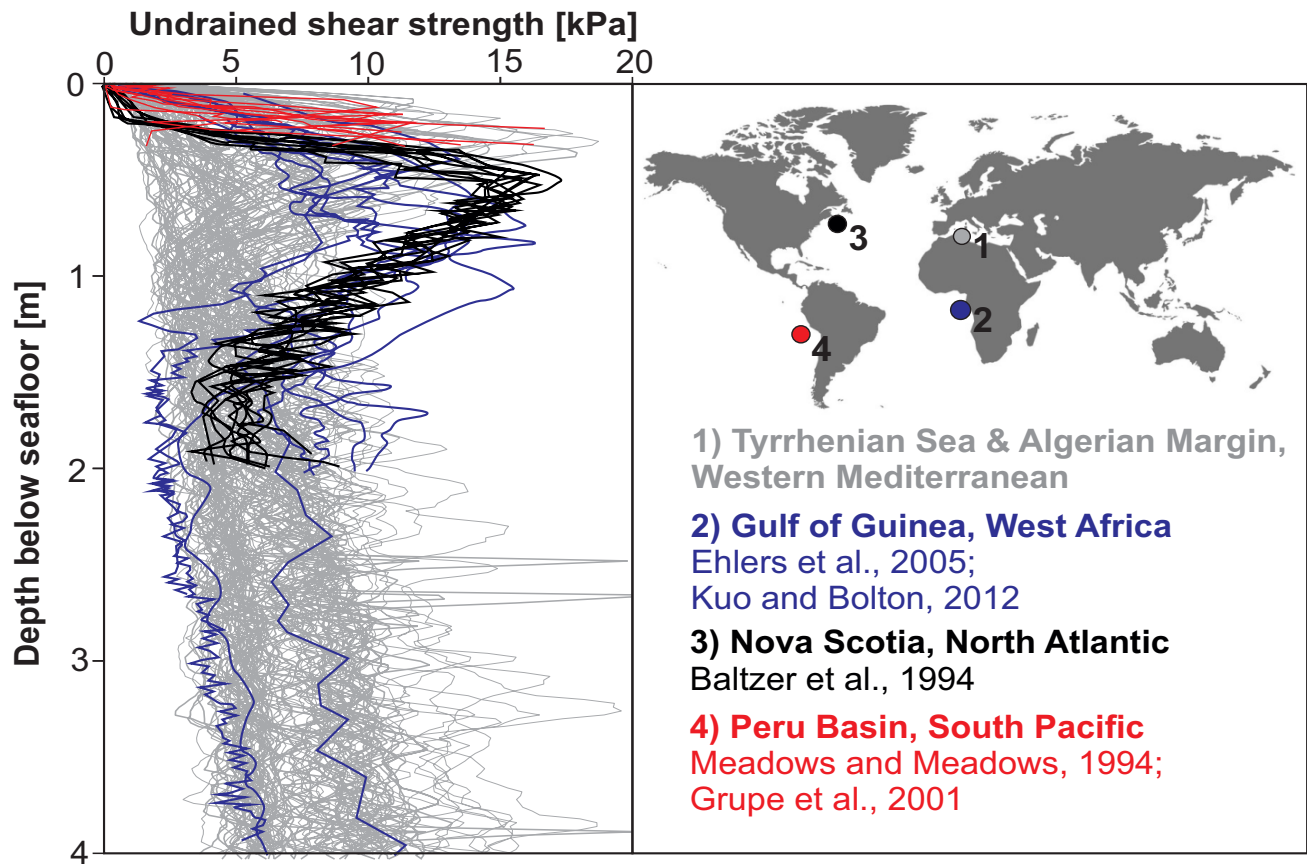
FIG. 9.—Summary figure showing **A**) a scenario where armored mud clasts are transported in a turbulent flow, the transformation of the flow into a debris flow, and **B**)

where armor can or cannot develop on a submarine fan, as well as the preservation of armored clasts in the linked debrite.

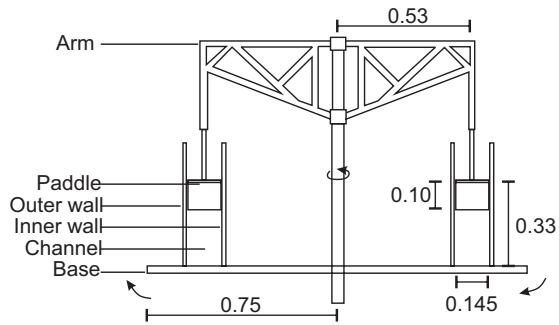
TABLE 1.—Comparison of mud-clast travel distances relative to their armored state, clast size trends, and inferred flow types.

Ancient Examples						
Geographical Location	Travel Distance	Armoring	Clast Size Trends	Inferred Flow Type	References	
Annot sandstone, France	Thought to be several kilometers. Origin of clasts unknown.	Armored	Up to 80 cm	Turbidity current	Stanley 1964	
Bed 1, Marnoso–Arenacea Formation, Italy	~ 40 km. Origin of clasts unknown.	Not mentioned	Decrease with distance. Clasts > 25 cm only extend up to 20 km along bed transect, smaller sizes extend to ~ 50 km along bed transect	Hybrid flow	Sumner et al. 2012	
Bed 5, Marnoso–Arenacea Formation, Italy	~ 10 km, possibly up to 80 km. Origin of clasts unknown.	Not mentioned	Clasts up to 10–25 cm diameter at 80 km along bed transect. Clasts > 25 cm cease after 20 km along bed transect	Hybrid flow	Sumner et al. 2012	
Outcrops	Huanghae Formation, China	Proximal to the slope failure region	Armored	20–40 cm	Debris flow	Chun et al. 2002
	Mayaro Formation, Trinidad	Unknown	Armored	Clast size not mentioned	Turbidity current	Dasgupta and Buatois 2012
	Miocene Austral Foreland Basin, Chile	Up to 700 m	Some armored	Up to 15 cm diameter	Turbidity current	Ponce and Carmona 2011
	Monterey Formation, California, USA	Unknown	Not mentioned	Clasts up to 1 cm diameter	Turbidity current or debris flow	Chang and Grimm 1999
	Oligocene Fusaru Sandstone and Lower Dysodilic Shale, Romania	Unknown	Not mentioned	Centimeter-scale	Turbidity current	Sylvester and Lowe 2004
	Polish Carpathians	Up to tens of kilometers	Some armored	Up to ~ 30 cm	Turbidity current	Felix et al. 2009

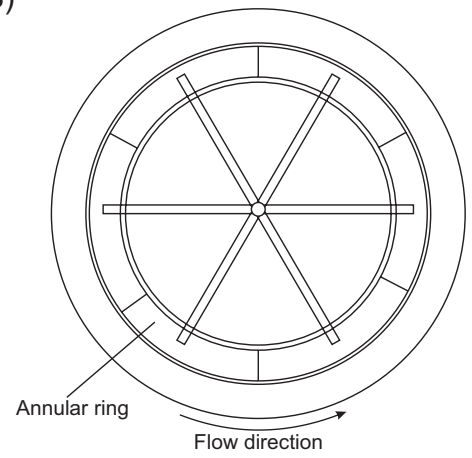
	West Crocker Fan, NW Borneo	Probably several tens of kilometers, although exact origin unknown.	Not mentioned	Up to 2 m in diameter	Turbidity current–debris flow	Jackson et al. 2009
Cores	Bed 5, Agadir basin, NW Africa	~ 25 km	Not mentioned	Clasts 5–10 cm in diameter	Hybrid flow	Stevenson et al. 2014; Sumner et al. 2012
	Britannia Formation, North Sea, UK continental shelf	Up to 100 km	Some armored	Clasts > 15 cm diameter	Hybrid flow	Haughton et al. 2003
Modern Examples						
	Geographical Location	Maximum Travel Distance	Armoring	Clast Size Trends	Inferred Flow Type	References
Cores	Cook Strait, New Zealand	Unknown	Not mentioned	Clasts < 5 cm in diameter	Turbidity current	Panti 1967
	Grand Banks deposit, Newfoundland, Canada	> 100 km	Armored	Clasts < 7 cm in diameter	Turbidity current	Stevenson et al. 2018
	Sur Landslide, USA	Up to 100 km	Some armored	Clasts 5 cm in diameter	Debris flow	Gutmacher and Normark 2002



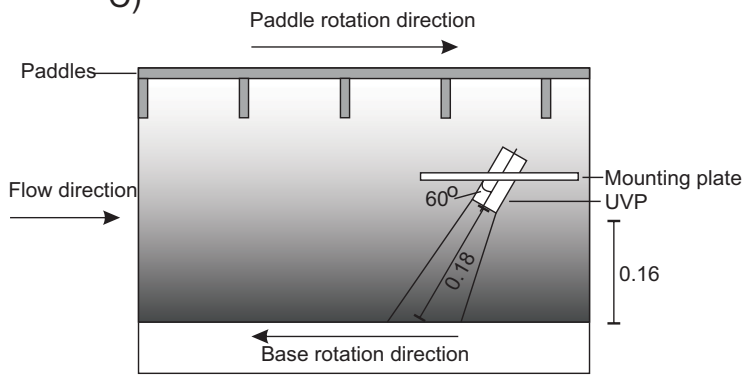
A)



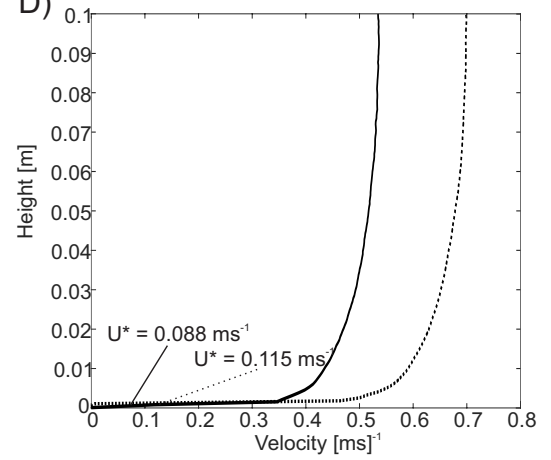
B)



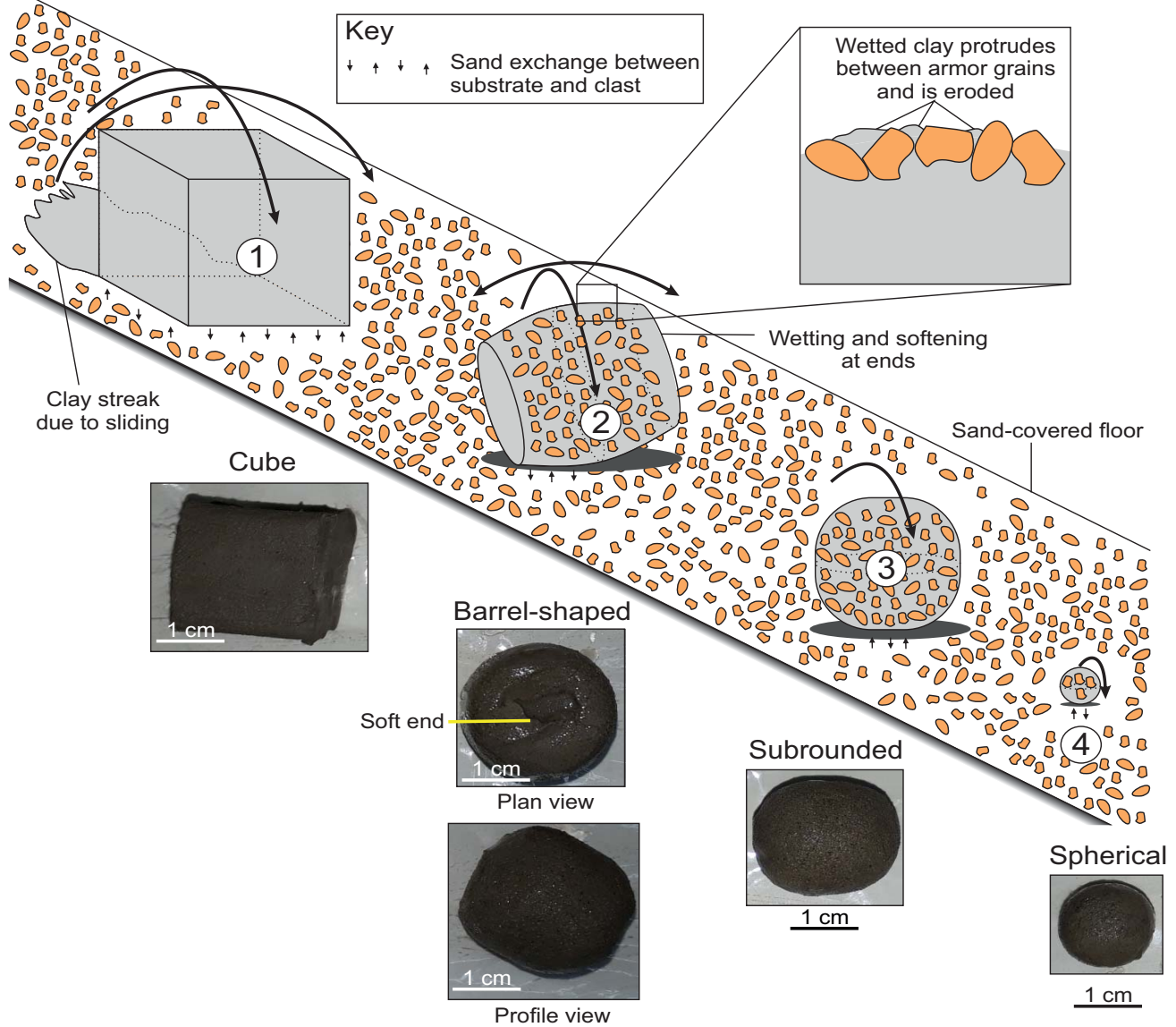
C)



D)



Clast Evolution



Stage 1: Cube

- Cube free to roll along either axis or slide along the bed
- Sand grains quickly adhere to the periphery of the clast as it rolls

Stage 2: Barrel-shape

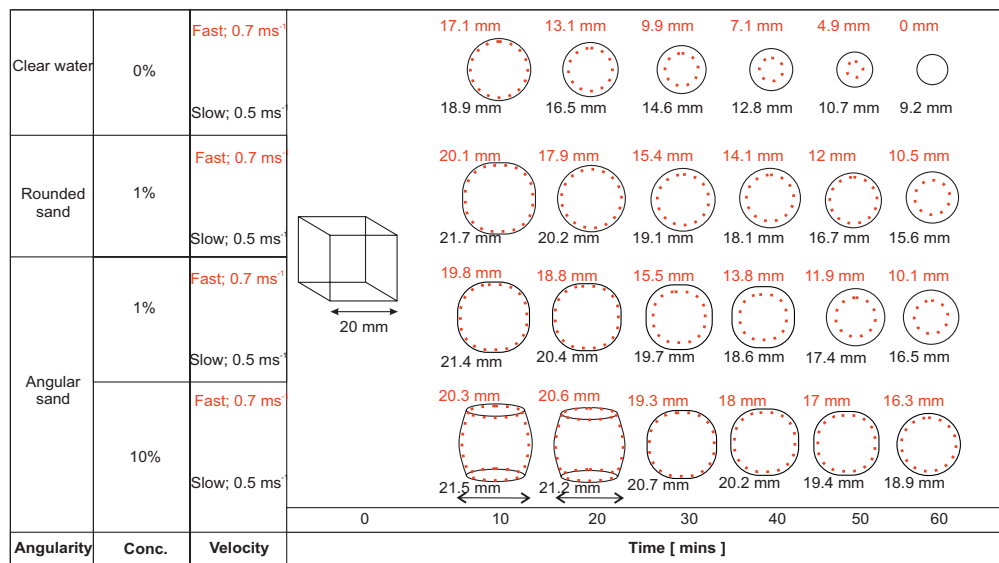
- Clast primarily rolls along minor axis
- Exchange of armor grains between the clast and the substrate as wetting occurs between grains
- Wet clay is extruded and eroded between armor grains and plucked as grains fall from clast

Stage 3: Subrounded

- Barrel-shaped clast becomes increasingly spherical as barrel ends are abraded
- Rolling along any axis promotes complete armoring
- Exchange of armor grains and mass loss via extrusion continues

Stage 4: Spherical

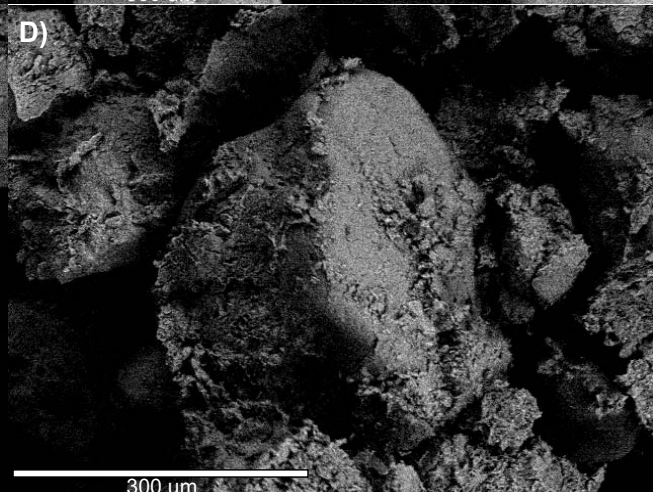
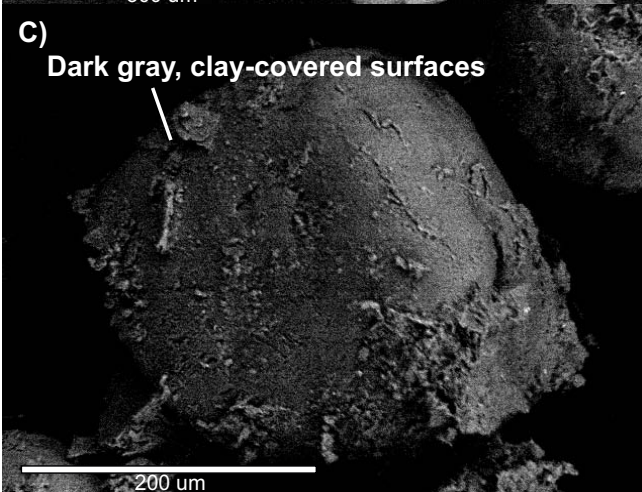
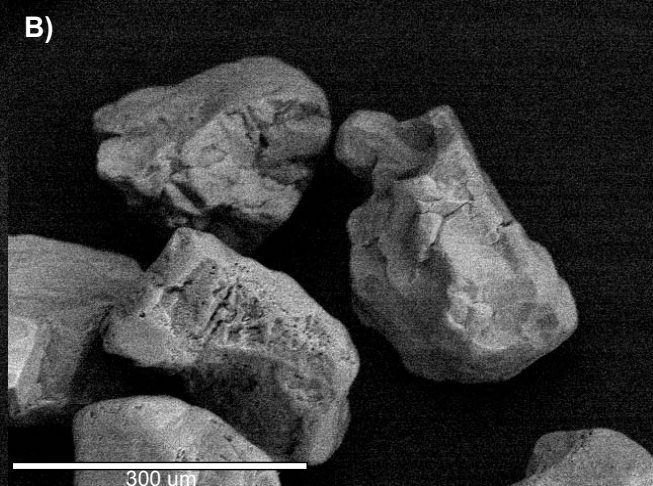
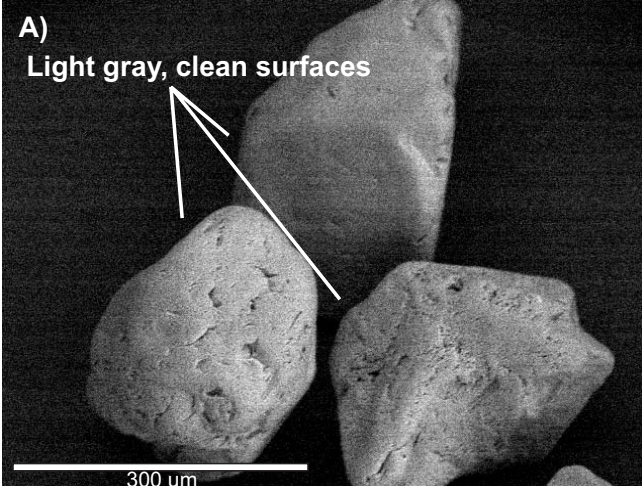
- Erosion slows as clast becomes smaller and rounder
- Exchange of armor grains and mass loss via extrusion continues
- Armor remains attached to the clast until it is completely abraded

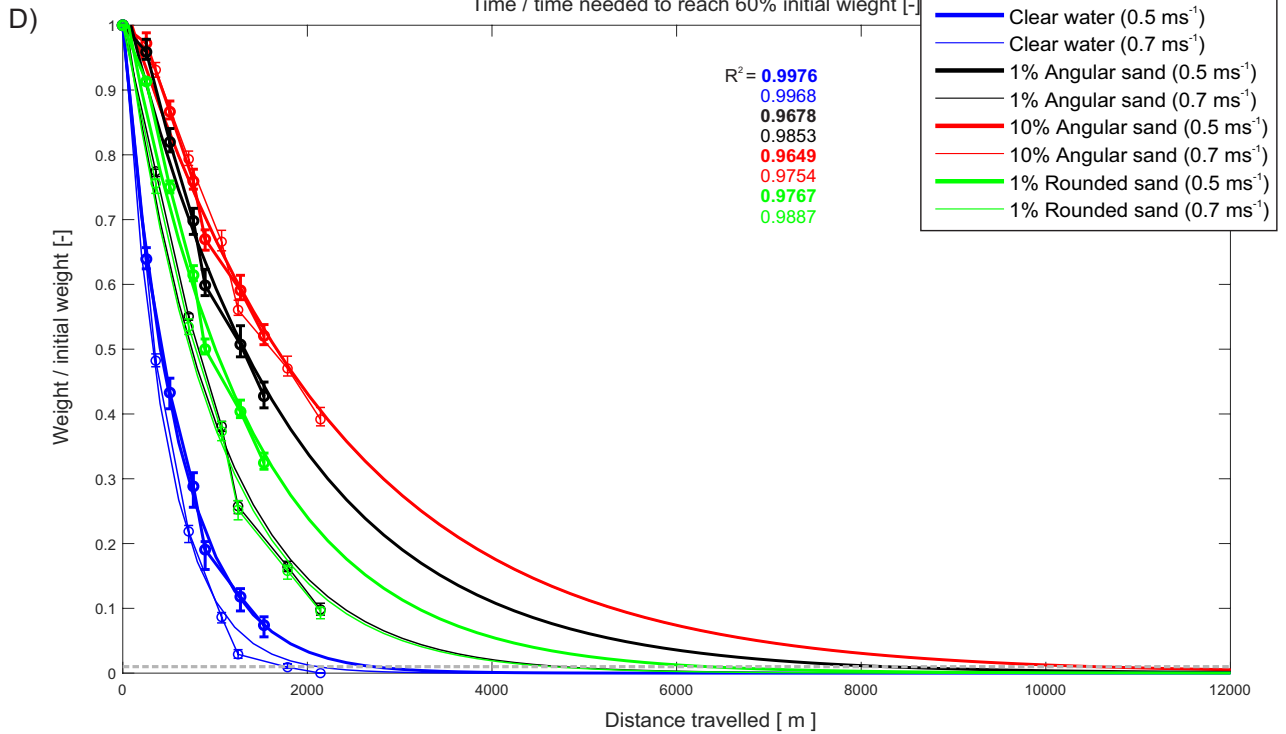
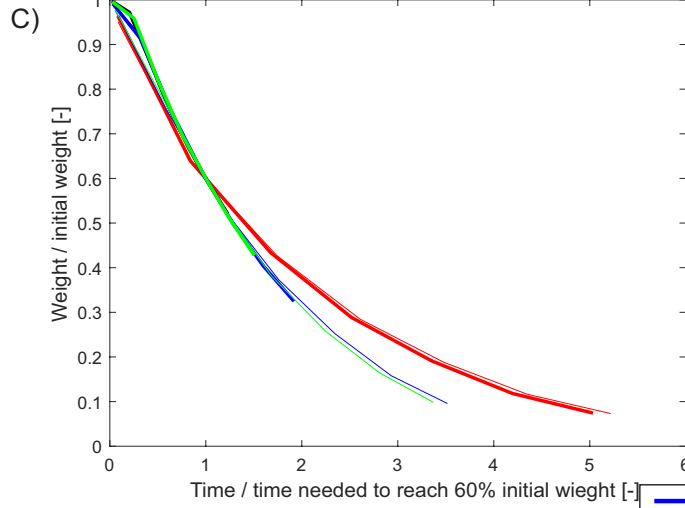
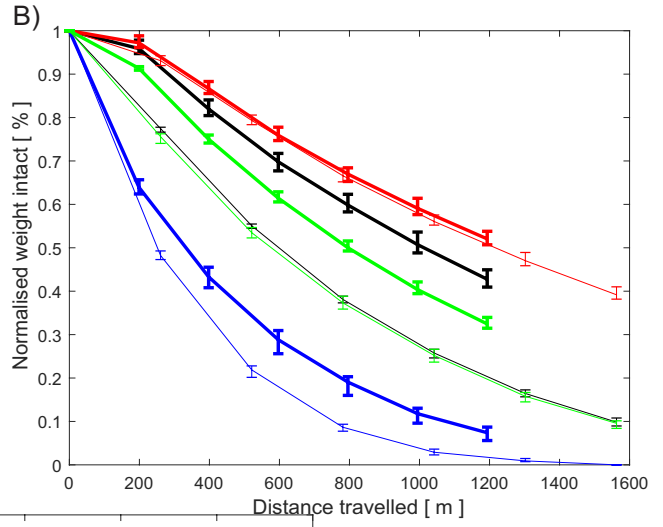
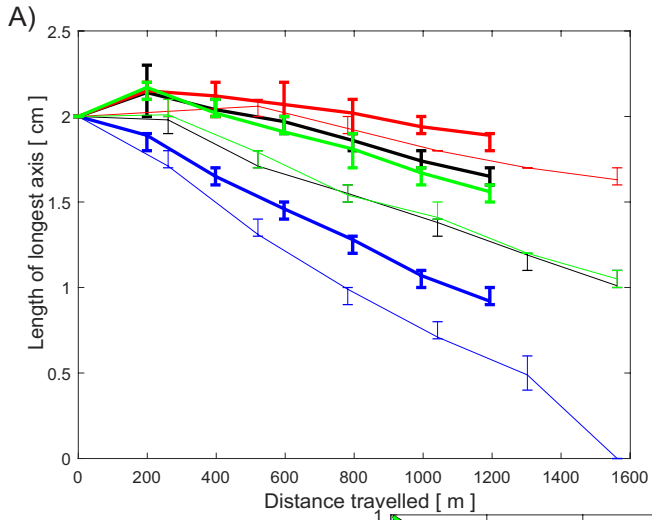


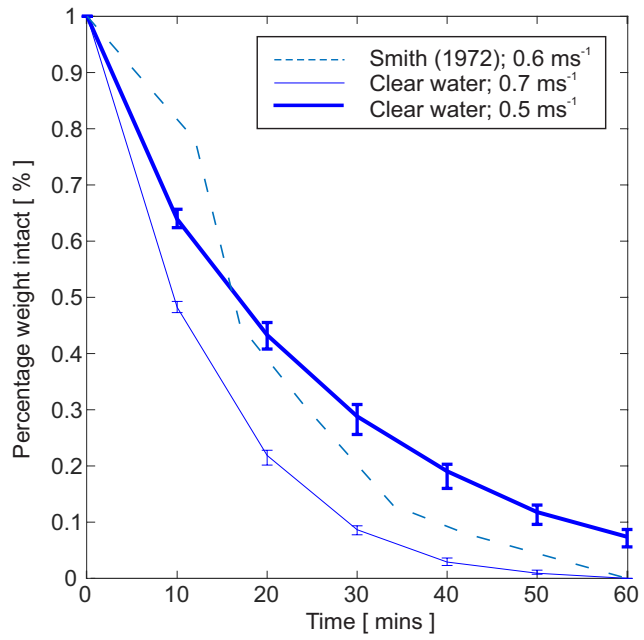
A)

B)

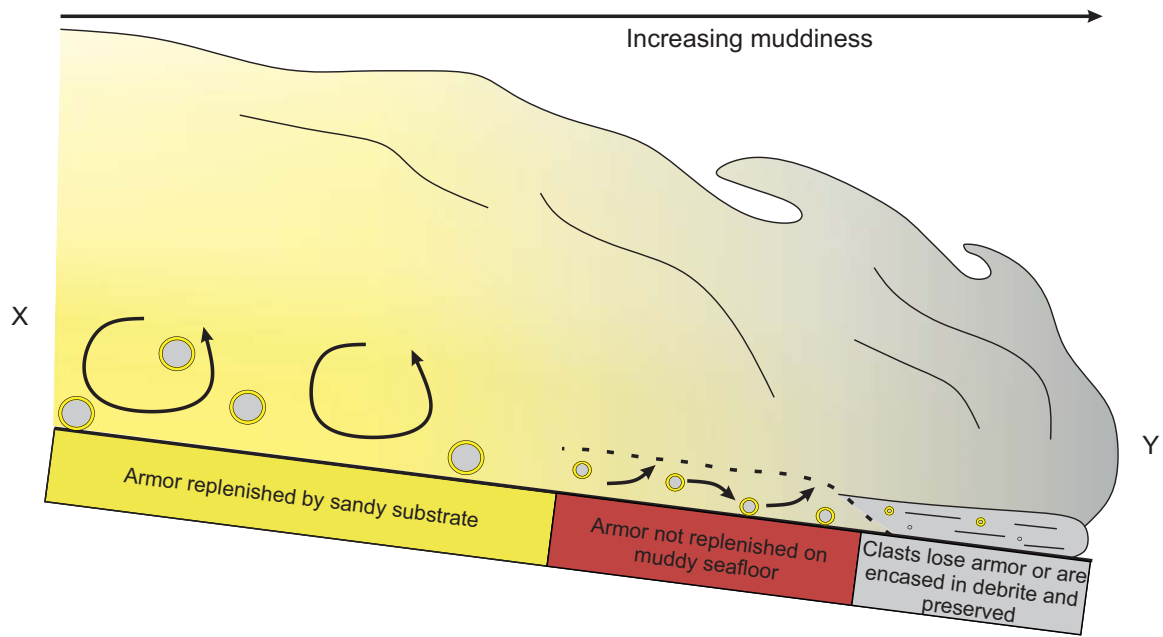








A) Clast armoring and flow transformation



B) Channel-lobe transition zone deposits and associated sediment logs

- Turbidite - sandy bed
- Transitional flow deposit - muddy bed
- Debrite - muddy bed

